MODIFIED EMBEDDED ATOM METHOD CALCULATIONS OF INTERFACES

M. I. Baskes

Sandia National Laboratories
Livermore, CA 94551-0969

Abstract

The Embedded Atom Method (EAM) is a semi-empirical calculational method developed a decade ago to calculate the properties of metallic systems. By including many-body effects this method has proven to be quite accurate in predicting bulk and surface properties of metals and alloys. Recent modifications have extended this applicability to a large number of elements in the periodic table. For example the modified EAM (MEAM) is able to include the bond-bending forces necessary to explain the elastic properties of semiconductors. This manuscript will briefly review the MEAM and its application to the binary systems discussed below.

Two specific examples of interface behavior will be highlighted to show the wide applicability of the method. In the first example a thin overlayer of nickel on silicon will be studied. Note that this example is representative of an important technological class of materials, a metal on a semiconductor. Both the structure of the Ni/Si interface and its mechanical properties will be presented. In the second example the system aluminum on sapphire will be examined. Again the class of materials is quite different, a metal on an ionic material. The calculated structure and energetics of a number of (111) Al layers on the (0001) surface of sapphire will be compared to recent experiments.

1. Introduction

The prominent use of composite materials in applications requiring an increased strength-to-weight ratio has made the development of these materials a critical technological issue. The behavior of these materials is often dominated by the properties of the interfaces inherent in them. For example, failure of even one of the numerous interfaces in engineering packaging applications can reduce reliability. In addition the understanding of metal-semiconductor interface structure is essential for a theoretical description of Schottky barrier heights[1]. Recently a number of continuum mechanics calculations have been performed to predict the mechanical behavior of composite materials[2]. Inherent in these calculations is an equation-of-state of the interface which has been assumed to be of a specific form (see e.g., Xu and Needleman[3] or Sherwood, et al.[4]). Such calculations have shown that the detailed behavior of the material at these interfaces frequently dominates the behavior of the composite as a whole. Hence, if these continuum computations are to be useful in predicting composite behavior, it is necessary to develop reliable models of the mechanical response of interfaces.

In order to calculate mechanical properties of specific interfaces an atomistic model is necessary. In this paper we choose to study two examples of the behavior of an interface between two dissimilar materials, a semiconductor and a metal and an ionic material and a metal. The systems chosen here for study are a thin overlayer of nickel on silicon and aluminum on sapphire (α-Al_2O_3). The Ni/Si system has important technological applications in the NiSi-Ni-Au contacting system to high-power silicon devices and as medium-barrier-height materials for high-power and signal-level silicon Schottky barrier diodes[5]. We have previously presented calculations on the Ni/Si system [6]. The Al/Al_2O_3 system represents an

important natural oxide system that forms as a protective coating for aluminum. In addition sapphire is commonly used as a substrate for many materials in the electronics industry. As a consequence a number of computational[7-9] and experimental[10, 11] studies of metal/sapphire interfaces have recently been performed.

In this work the Modified Embedded Atom Method (MEAM) developed by Baskes et al. [12-14] is used to calculate the geometry and energetics of a thin metal overlayer on various substrates. The MEAM follows the EAM concept [15, 16] in that the energy of a given atom is taken as one half the energy in two-body bonds with its neighboring atoms plus the energy to embed the atom in the electron density at its site arising from all the other atoms. In the EAM, this background electron density is a simple sum of radially dependent contributions from the other atoms, while in the MEAM the background electron density includes angular dependence. Also, the most recent implementation of the MEAM[14] incorporates a strong screening function so that the model is very short ranged for a structure that is reasonably tight packed, but can be long ranged in open structures such as at a surface. MEAM potentials are now available [14, 17] for 44 elements in the periodic table including materials with fcc, bcc, hcp, and diamond cubic crystal structures.

It is assumed in the MEAM[14] that the energy per atom is a known function of the nearest-neighbor distance in the reference structure for the element under consideration. An analytic form for the electron density at a given atom site arising from the other atoms and an analytic form for the embedding energy as a function of the electron density are assumed. These equations imply the analytic form that the two-body potential must have as a function of the nearest-neighbor distance in the reference lattice. This form is then adopted for general use, i.e., it is taken as the two-body potential, as a function of separation distance, for any configuration or symmetry condition of the two-body bond.

In the body of the manuscript below we briefly review the underlying equations of the MEAM, demonstrate its application to the Si-Ni and Al-O systems, and present the results for the thin overlayer of nickel on silicon and aluminum on sapphire. We conclude with a short summary.

2. Theory

The Modified Embedded Atom Method (MEAM) has been fully discussed previously[12-14] and will only be briefly reviewed here. The general energy expression of both the EAM and MEAM can be written as:

$$E = \sum_i \left[F_i\left(\bar{\rho}_i\right) + \frac{1}{2}\sum_{j \neq i} \varphi_{ij}\left(R_{ij}\right) \right] \tag{1}$$

where E represents the energy of an assemblage of atoms i, F_i is the embedding function for atom i embedded in a background electron density $\bar{\rho}$, and ϕ_{ij} is the pair potential between atoms i and j separated by a distance R_{ij}.

In the EAM the background electron density is taken to be a linear superposition of the spherically averaged atomic electron densities, $\rho^{(0)}$. In contrast in the MEAM angular effects are taken into account. The effect of the angular terms is captured by one variable, Γ, given by:

$$\Gamma = \sum_{l=1}^{3} t^{(l)}\left(\rho^{(l)}/\rho^{(0)}\right)^2 \tag{2}$$

where $\rho^{(l)}$ is the partial electron density as defined in Baskes[14] and $t^{(l)}$ are constants.

For the Ni/Si system the background electron density is given by:

$$\overline{\rho} = \rho^{(0)}\sqrt{1+\Gamma} \tag{3a}$$

and for the Al/O system:

$$\overline{\rho} = \rho^{(0)}\frac{2}{1+e^{-\Gamma}} \tag{3b}$$

Both of these forms yield the same asymptotic expression for the background electron density in the limit of small angular contributions. The first expression Eq. (3a) leads to computational problems for large negative Γ.

3. Application to the Ni/Si and Al/O Systems

The MEAM potentials for silicon, nickel, aluminum, and oxygen have been previously developed [14]. We will use the potentials for silicon and nickel without modification as in Baskes et al. [6]. The parameters for aluminum have been modified to account for a more recent experimental value of the sublimation energy[18] and those for oxygen have been modified to reproduce the oxygen trimer better. The parameters for these potentials are given in Table 1. Definitions for the parameters may be found in Reference [14].

Table 1: Parameters for the MEAM. Values listed are the cohesive energy E_c (eV), the equilibrium nearest neighbor distance r_e (Å), the exponential decay factor for the universal energy function α, the scaling factor for the embedding energy A, the exponential decay factors for the atomic densities $\beta^{(i)}$, the weighting factors for the atomic densities $t^{(i)}$, and the atomic density scaling ρ_0.

	E_c	r_e	α	A	$\beta^{(0)}$	$\beta^{(1)}$	$\beta^{(2)}$	$\beta^{(3)}$	$t^{(1)}$	$t^{(2)}$	$t^{(3)}$	ρ_0
Ni	4.450	2.49	4.99	1.10	2.45	2.20	6.00	2.2	3.57	1.60	3.70	1.00
Si	4.630	2.35	4.87	1.00	4.40	5.50	5.50	5.5	3.13	4.47	-1.80	2.05
Al	3.360	2.86	4.61	1.10	1.26	4.35	7.00	2.2	-0.34	-1.69	8.30	0.40
O	2.558	1.21	4.59	0.80	2.31	2.26	2.07	1.52	11.80	8.40	-6.20	1.30

The modified embedded atom method has been applied by Baskes et al. [6] to two phases of the Si-Ni system for which a significant amount of experimental information is available. The first phase, Ni_3Si, which has a $L1_2$ structure, is used as the reference structure for determining the cross potentials between the nickel and silicon. The second phase considered is the $NiSi_2$ phase. This phase is important in studies of Ni/Si thin film structures since it is found to form when nickel is deposited onto silicon by molecular beam epitaxy [19]. The resultant parameters are given in Table 2.

Table 2: Parameters for the MEAM alloy reference structures. Values listed are the cohesive energy E_c (eV), the equilibrium nearest neighbor distance r_e (Å), and the exponential decay factor for the universal energy function α.

	crystal structure	E_c	r_e	α
Ni_3Si	$L1_2$	4.855	2.42	6.0
AlO	B1	4.000	1.97	4.5

It is necessary to choose a reference structure for the Al/O system in order to determine the Al-O pair interaction. The choice of the reference structure is arbitrary, the assumption in the model being that results are independent of this choice. In the past we have used the equilibrium structure of an experimentally accessible compound for the reference structure. For the Al/O system, however, the equilibrium structures are complex. In order to maintain simplicity, the reference structure is chosen as the B1 (NaCl) structure rather than the complex α phase Al_2O_3. Total energy first principles calculations [20] of the B1 phase as a function of lattice parameter are used to determine the equation of state. The lattice parameters and internal coordinates of the α phase are also fit using the oxygen electron density decay parameters and the electron density scaling.

3.1 Verification of the model

To examine the accuracy of the model a number of simple calculations were performed for Ni-Si and Al-O compounds. The results are summarized in Table 3. The first six rows of this table are the results of the fitting procedure described above. The structural properties of the compounds are described well, including the internal coordinates which determine the atom positions in the complex sapphire structure. All of the other values listed in Table 3 are predictions. The elastic constants were determined using the numerical evaluation procedure described in reference [13]. The results for Ni_3Si are in good agreement with first principles calculations differing by at most 20 percent for C_{44}. For $NiSi_2$ our results are in fair agreement with the LMTO calculations of Lambrecht et al.[21] who reported a bulk modulus of 160 GPa compared to our calculated value of 224 GPa. We may also compare to the tight-binding calculations of Malegori and Miglio[22] who reported a value of C_{11}-C_{12} of 58 GPa compared to our calculated value of 45 GPa. It should be noted that in the calculation of C_{44} for $NiSi_2$ and all of the Al_2O_3 elastic constants, the lattice exhibited an internal relaxation similar to that observed in diamond cubic materials[13, 23]. These relaxations are significant and perhaps are responsible for the only fair agreement of the Al_2O_3 predicted elastic constants. Streitz and Mintmire[8, 9] fit their potentials to the unrelaxed elastic constants, but did not calculate the relaxed values. The shear elastic constants for AlO are not given since our calculations show that AlO is unstable with respect to shear. There is no problem in the model in having a reference structure being unstable. Reference [6] contains a complete discussion of the computational details and the comparison to experiment for the Ni/Si planar defects listed in Table 3.

There are three possible terminations of (0001) sapphire. We find that the oxygen terminated sapphire (0001) surface has the lowest surface energy, followed by the double Al layered termination. These results are in agreement with experiment[10, 11] and in conflict with first principles calculations[24]. The surface energy and hence fracture energy calculated here for the sapphire (0001) surface is significantly higher than the fracture energy derived from surface energies reported in previous empirical and first principles calculations[8, 9, 34, 35].

4. Results and Discussion

4.1 Nickel on Silicon

The modified embedded atom method (MEAM) was applied to the study of a thin 10 Å layer of Ni on Si(001)[6]. The nickel was expanded by about nine percent so as to be lattice matched to the silicon substrate. Once the ideal boundary structure was created it was

Table 3: Calculated properties of $NiSi_2$, Ni_3Si, AlO, and Al_2O_3. For comparison experimental data or first principles calculations are shown in parentheses.

Property	Calculation			
	$NiSi_2$	Ni_3Si	AlO	Al_2O_3
Cohesive Energy (eV/atom)	4.92 (4.88)	4.855 (4.855[a])	4.0 (4.0[b])	6.04 (6.3[c])
Lattice Constant a_0(Å)	5.404 (5.38-5.406[d])	3.504 (3.505-3.510[d])	3.94 (4.44[b])	4.61 (4.758[e])
Lattice Constant c_0 (Å)				12.88 (12.99[e])
Bulk Modulus (GPa)	224 (160[f])	288 (254-262[g])	188 (132[b])	
Internal Coordinate, u				0.27 (0.30[e])
Internal Coordinate, v				0.36 (0.35[e])
C_{11} (GPa)	254	389 (363-375[g])		359 (494[h])
C_{12} (GPa)	209	237 (200-205[g])		279 (158[h])
C_{44} (GPa)	18.3	202 (167-172[g])		116 (145[h])
C_{33} (GPa)				230 (496[h])
C_{13} (GPa)				82 (114[h])
C_{14} (GPa)				-21 (-23[h])
(111) Fracture Energy (J/m^2)	8.7, 7.0	4.4 (5.1[i])		11.4[j]
(100) Fracture Energy (J/m^2)	6.5	5.2 (7.2[i])		
(111) APB (mJ/m^2)		844 (625-676[h],250[k])		
(100) APB (mJ/m^2)		95 (670-707[h],250[k])		
(111) CSF (mJ/m^2)		872 (710[l])		
(111) SISF (mJ/m^2)		283 (460[l])		

[a] Reference [25]
[b] Reference [20] first principles calculations
[c] Reference [28]
[d] Reference [30]
[e] Reference [31]
[f] Reference [21] first principles calculations
[g] Reference [26] first principles calculations
[h] Reference [27]
[i] Reference [29] first principles calculations
[j] (0001) between O and Al planes
[k] Reference [32]
[l] Reference [33] first principles calculations

minimized using a conjugate gradient method. Upon minimization the nickel atoms near the interface showed a rippled structure with some of the atoms moving away from the interface and some moving toward the interface. The maximum extent of the rippling was approximately 0.12 Å which occurred at the interface. The source of the rippling appeared to be the presence or absence of silicon atoms directly below the nickel atoms at the interface.

The minimized interface structure was then separated to determine the work of adhesion. The lattices were separated using two different methods in order to estimate the effects of lattice relaxation during separation. The first was used to determine the ideal work of adhesion which is just the difference in energy between the interface structure and the separated crystals. This determination was accomplished by separating the lattices in 0.4 Å steps with the unrelaxed (no atom motion except for the rigid separation) energy being

calculated at each step. The resultant energy/displacement curve is indicated by the triangles in Figure 1. The x axis shows the displacement of the surface nickel atoms from their position in the minimized energy configuration. The y axis shows the difference in energy between the separated structure and the initial interface structure. For this case the energy of the system increases monotonically to approximately 6.4 J/m^2 above that for the minimized interface structure. The curve shows a peak in the energy of the system at a separation of approximately 2.5 Å with a small decrease in energy upon further separation. When the nickel and silicon have been separated beyond 3 Å, the energy of the system is essentially unchanged with only small differences in the calculated energy caused by weak overlap of the electron density tails.

The second method for calculating the work of adhesion was to separate the lattice by 0.4 A, as in the previous case, but to minimize the energy via atomic motion before the next step in the separation. This method represents quasi-static separation of the thin layer. For this case the surface layer of nickel atoms was held fixed at the separated distance but the atoms were allowed to move within the surface plane. This method of separation produced the relaxed energy curve, indicated by the open squares, shown in Figure 1. In this case, the lattices separated much further before the interface failed. This effect occurs because much of the work applied to the interface structure was absorbed as strain energy. A difference between the relaxed and the rigid curves is that with relaxation the energy increased monotonically with separation until the boundary catastrophically failed. When the boundary failed the strain energy was released causing the energy of the system to drop dramatically. In fact the energy of the system in this case was much lower after failure of the boundary as compared to the previous case predicting a relaxed work of adhesion of 1.5 J/m^2. There are two reasons that this work of adhesion is much lower. The first and most significant, is that the separation did not occur exactly at the interface, i.e., a layer of silicon atoms stayed attached to the nickel layer upon failure of the interface. This layer of silicon atoms which was stuck to the nickel lattice was strongly bound with binding energies larger than silicon atoms one or two layers away from a Si surface. This new surface was responsible for about 70% of the reduction in the work of adhesion. In addition, after separation the atoms at the new surfaces, which were created when the boundary failed, were allowed to relax. For the silicon surface, the relaxation produced a 2x1 reconstruction in agreement with experiment[36]. The Si surface relaxations further lowered the energy by about 0.4 eV/surface atom or 30% of the lowering of the work of adhesion.

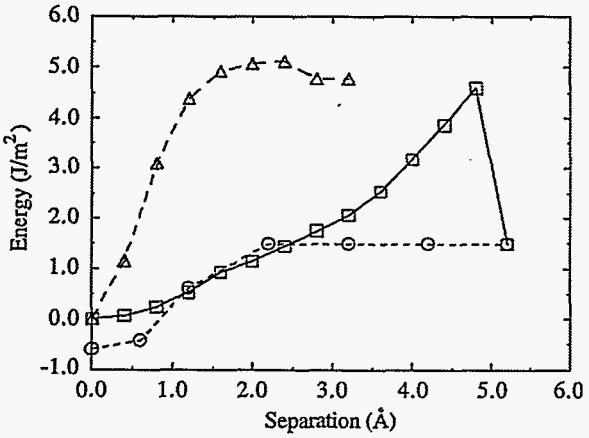

Fig. 1 The energy, measured relative to the initial minimized structure, of the system as a function of separation. The curve indicated by the triangles is the energy calculated when the lattices were rigidly separated with no atomic relaxations. The curve indicated by the open squares is the energy of the system during the separation process when the atoms are allowed to reach a minimum energy configuration at each step of separation. The last curve indicated by the circles is the energy of the system when the lattices were rejoined.

The separated crystals were then rejoined by moving them together in 1.0 Å steps, with the energy being minimized at each step. No interaction between the crystals was observed until the lattices reached a separation of 3.2 Å (Figure 1). At this separation the energy of the system is

10 mJ/m^{2}less than when the crystals are separated by more than this distance. The energy of the system drops as the crystal halves are brought closer together since the surface atoms begin to interact more strongly. The reason the energy of the system decreases to below that of the initial interface structure, by approximately 0.6 J/m^2, is due to a breaking of symmetry upon reaffixing the crystal halves.

4.2 Aluminum on Sapphire

The initial stages of growth of aluminum on sapphire substrates have recently been studied by Medlin et al. [37]. In this work it is found that there are three preferred orientations of (111) textured Al on the (0001) sapphire. In order to investigate the orientation dependence of Al on sapphire, cylindrical islands (16 Å diameter) of (111) Al were placed on the oxygen terminated (0001) relaxed sapphire surface (see Figure 2). An island geometry was chosen to avoid the computational problems associated with the misfit between the aluminum and sapphire lattices. The islands were 10 Å thick and spaced ~25 Å apart. A number of island orientations and initial displacements were chosen. The top plane of the Al island was held fixed in the plane of the surface, but was allowed to move normal to the surface. Similarly the bottom few planes of the sapphire substrate were held fixed. All of the other atoms were allowed to relax to their equilibrium positions. The resultant energies relative to the lowest energy interface are given in Figure 3. We find that there are four orientations (0°, ~14°, ~24°, and 30°) that have significantly lower energies than the other orientations. These results compare favorably to experiment where three preferred angles (0°, ~11°, and 30°) are found. It is possible that complete relaxation of the island, i.e. removing the constraint of the top Al layer, would show that the orientation not seen in experiment is metastable. Such calculations are in progress.

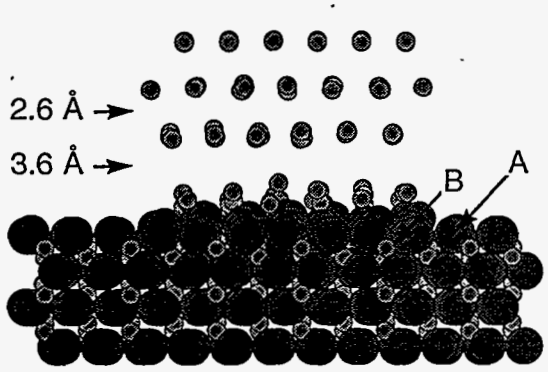

Fig. 2 Atomic positions of a single (111) Al (small circles) island on a (0001) sapphire surface. Terminating plane types are indicated by A for the O plane and B for the Al plane. The spacing of the first two Al layers at the interface is significantly greater that that in the rest of the Al overlayer.

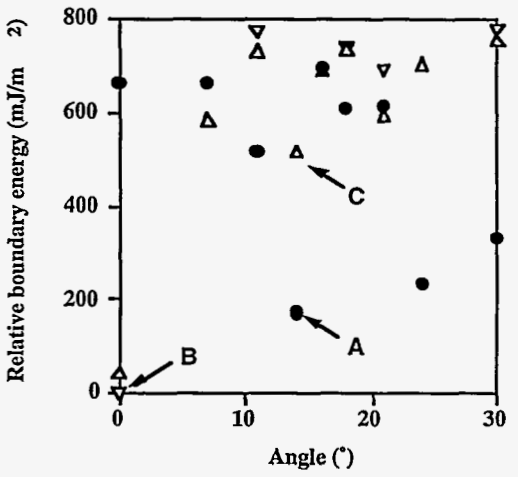

Fig. 3 Relative boundary energies of (111) Al clusters on (0001) sapphire as a function of rotation angle about the surface normal. The angle is defined to be zero for $[1\bar{1}0]\mathrm{Al} \parallel [10\bar{1}0]\mathrm{Al_2O_3}$. The letters A (filled circle) and B, C (open triangles) represent the in-plane displacement of the Al cylinder relative to the substrate.

The calculations show that for the 0° orientation the Al atoms are located above the Al atoms just below the terminal oxygen plane of the sapphire (denoted B in the figure). For the other three preferred orientations, the Al cylinder is shifted so that an Al atom is located directly above an oxygen in the terminal plane (denoted A in the figure). We also find (see Figure 2) that the spacing of the Al planes at the interface varies significantly with the first two planes at the interface separated by ~1 Å more than the more distant planes that take on a spacing ~0.3 Å greater than the bulk Al (111) spacing. Direct comparisons with high resolution electron microscopy are in progress.

We would expect that the interface would be weakest where the Al spacing is increased. Preliminary calculations show that as expected the interface fractures with the first Al plane attached to the sapphire substrate similarly to the fracture of the Ni/Si system discussed above. In this case however, it is the overlayer plane that is attached rather than the substrate plane.

5. Summary

The MEAM has been applied to the calculation of the structure and energy of a thin metallic layer of Ni on Si and Al on sapphire. This empirical method of calculation is an extension of the EAM which includes angular forces necessary to describe the bonding of covalent materials such as Si and ionic materials such as sapphire. The MEAM formalism has been described and applied to the Si-Ni and Al-O systems. A number of simple properties such as elastic constants, surface energies, and fault energies, of four compound phases are calculated and compared to experiment and first principles calculations. In general the results are satisfactory.

Our calculations predict two low energy Si-Ni interface structures both of which have a slightly rippled Ni structure. The lower energy interface also contains rows of shifted Ni atoms. The MEAM potentials predict significant differences between the ideal unrelaxed (4.8 J/m^2) and relaxed (1.5 J/m^2) work of adhesion of the thin nickel overlayer on Si(001). This large difference is attributed to 1) variation in the plane of fracture from that between the Si and Ni lattices to between the two Si planes nearest the interface; and 2) reconstruction of the fractured Si surface to a 2x1 structure.

Four low energy orientations of (111) Al clusters on (0001) sapphire were found in good agreement with the three orientations found by experiment. Two of the configurations at 0° and 30° are identical. Investigation of the equilibrium structure of the (111) Al layers at the interface showed an ~1 Å increase in interplanar spacing between two specific layers. This structure results in fracture between these Al layers rather than at the interface.

Acknowledgment

This work was supported by the USDOE.

References

1. J. Bardeen, Phys. Rev. **71**, (1947) 717.
2. Mechanics of Material Interfaces, A. P. S. Selvadurai, G. Z. Voyiadjis, Eds., ASCE/ASME Mechanics Conference, Alburquerque, NM (Amsterdam: Elsevier, 1985).
3. X.-P. Xu, A. Needleman, Modelling Simul. Mater. Sci. Eng. **1**, (1993) 111.
4. J. A. Sherwood, H. M. Quimby, R. J. Doore, Damage Modeling in Fiber Reinforced Composites, A. Nagar, Ed., Winter Annual Meeting of the American Society of

Mechanical Engineers, Anaheim, CA (American Society of Mechanical Engineers, 1992).
5. D. J. Coe, E. H. Rhoderick, J. Phys. D: Appl. Phys. **9**, (1976) 965.
6. M. I. Baskes, J. E. Angelo, C. L. Bisson, Modelling Simul. Mater. Sci. Eng. **2**, (1994) 505.
7. P. Alemany, R. S. Boorse, J. M. Burlitch, R. Hoffmann, J. Phys. Chem. **97**, (1993) 8464.
8. F. H. Streitz, J. W. Mintmire, Composite Interfaces **2**, (1994) 473.
9. F. H. Streitz, J. W. Mintmire, Phys. Rev. B **50**, (1994) 11996.
10. M. Gautier, et al., J. Am. Ceram. Soc. **77**, (1994) 323.
11. M. Vermeersch, F. Malengreau, R. Sporken, R. Caudano, Surf. Sci. **323**, (1995) 175.
12. M. I. Baskes, Phys. Rev. Lett. **59**, (1987) 2666.
13. M. I. Baskes, J. S. Nelson, A. F. Wright, Phys. Rev. B **40**, (1989) 6085.
14. M. I. Baskes, Phys. Rev. B **46**, (1992) 2727.
15. M. S. Daw, M. I. Baskes, Phys. Rev. Lett. **50**, (1983) 1285.
16. M. S. Daw, M. I. Baskes, Phys. Rev. B **29**, (1984) 6443.
17. M. I. Baskes, R. A. Johnson, Modelling Simul. Mater. Sci. Eng. **2**, (1994) 147.
18. R. C. Weast, Ed., *Handbook of Chemistry and Physics* (CRC, Boca Raton, FL, 1984).
19. R. T. Tung, J. M. Gibson, J. M. Poate, Phys. Rev. Lett. **50**, (1983) 429.
20. D. A. Papaconstantopoulos, private communication, 1995.
21. W. R. L. Lambrecht, N. E. Christensen, P. Blöchl, Phys. Rev. B **36**, (1987) 2493.
22. G. Malegori, L. Miglio, Phys. Rev. B **48**, (1993) 9223.
23. R. A. Johnson, Modelling Simul. Mater. Sci. Eng. **1**, (1993) 717.
24. J. Guo, D. E. Ellis, D. J. Lam, Phys. Rev. B **45**, (1992) 13647.
25. F. R. de Boer, R. Boom, W. C. M. Mattens, A. R. Miedema, A. K. Niessen, *Cohesion in Metals Transition Metal Alloys*. F. R. de Boer, D. G. Pettifor, Eds., Cohesion and Structure (North-Holland, Amsterdam, 1988), vol. 1.
26. C. L. Fu, Y. Y. Ye, M. H. Yoo, Phil. Mag. Lett. **67**, (1993) 179.
27. K.-H. Hellwege, Ed., *Landolt-Börnstein Numerical Data and Functional Relationships in Science and Technology*, vol. 1 (Springer-Verlag, Berlin, 1966).
28. E. A. Brandes, Ed., *Smithells Metals Reference Book* (Butterworths, London, 1983).
29. M. H. Yoo, C. L. Fu, Mater. Sci. Eng. A **153**, (1992) 470.
30. P. Villars, L. D. Calvert, *Pearson's Handbook of Crystallographic Data for Intermetallic Phases* (ASM International, Materials Park, OH, 1991), vol. 4.
31. P. Villars, L. D. Calvert, *Pearson's Handbook of Crystallographic Data for Intermetallic Phases* (ASM International, Materials Park, OH, 1991), vol. 1.
32. B. Tounsi, Ph. D., University of Poitiers (1988).
33. M. H. Yoo, C. L. Fu, J. A. Horton, Mater. Sci. Eng. A **176**, (1994) 431.
34. I. Manassidis, A. DeVita, M. J. Gillan, Surf. Sci. Lett. **285**, (1993) L517.
35. I. Manassidis, M. J. Gillan, J. Am. Ceram. Soc. **77**, (1994) 335.
36. R. M. Tromp, R. J. Hamers, J. E. Demuth, Phys. Rev. Lett. **55**, (1985) 1303.
37. D. L. Medlin, et al., submitted for publication , (1996) .

DISCLAIMER